

N-Acetylbenzotriazole Hydrolysis and Aminolysis. Brønsted Relationships and Rate-Determining Steps in the Uncatalyzed and Catalyzed Aminolysis

Michèle Reboud-Ravaux

Contribution from the Laboratoire de Chimie Organique Biologique, Bâtiment 420, Centre d'Orsay, Université de Paris-XI, 91405 Orsay Cedex, France.
Received June 20, 1979

Abstract: The hydrolysis of *N*-acetylbenzotriazole is pH independent in the pH range 2.5–6 and catalyzed by hydroxide ion at higher pH. Based on the solvent deuterium isotope effect, the value of entropy of activation, and structure–reactivity considerations, a mechanism involving at least two water molecules in the transition state is proposed for the pH-independent hydrolysis. *N*-Acetylbenzotriazole exhibits little susceptibility to catalysis by proton and acids. Catalysis by weak acids is attributed to general base catalysis of hydrolysis (Brønsted β value = 0.38). Curved Brønsted plots were obtained for both general acid and general base catalysis of methoxyaminolysis with limiting slopes approaching 0 for strong catalysts and 1 or –1 for weak ones. These observations suggest that general acid and general base catalysis involve a kinetically significant proton-transfer step. Possible mechanisms involving intermediates that are not at equilibrium with respect to proton transfer and their relationship to the lifetime of these intermediates and the position of the breaks in the Brønsted plots are described. The rate constants for the uncatalyzed aminolysis by a series of amines increase sharply with increasing amine basicity ($\beta_{\text{nuc}} = 1.0$); the rate-determining step is attributed to the uncatalyzed breakdown of the addition intermediate T^\ddagger . Catalysis of aminolysis by a second molecule of amine is characterized by a Brønsted plot of slope equal to 0.86. Surprisingly, all the absolute rate constants obtained with *N*-acetylbenzotriazole are considerably slower than that expected from the pK_a of benzotriazole if compared to acetylimidazole and 1-acetyl-1,2,4-triazole, especially for general-acid- and general-base-catalyzed pathways. The reasons and implications of this last result are discussed.

Introduction

Considerable interest has attached to the mechanism of general acid and general base catalysis of complex reactions in water, especially for general acid–base catalysis of carbonyl and acyl group reactions.^{1,2} The question of whether these reactions are concerted or proceed through tetrahedral intermediates is of continual concern. On the basis of nonlinear Brønsted plots, stepwise mechanisms have been suggested for both general acid and general base catalysis of methoxyaminolysis of 1-acetyl-1,2,4-triazole³ and for the general-base-catalyzed hydrazinolysis of *N*-acetylimidazole,⁴ with intermediates that are not at equilibrium with respect to transport processes. As a further illustration of such kinds of mechanisms for reactions involving *N*-acetylazoles, we describe here the characteristics of the uncatalyzed and catalyzed reactions of *N*-acetylbenzotriazole with water and amines. Results have shown appreciable differences from that obtained with 1-acetyl-1,2,4-triazole and the purpose of this paper is to point these out. A preliminary study of the hydrolysis of *N*-acetylbenzotriazole was reported⁵ and this amide was previously described as a protein reagent.⁶

Experimental Section

Materials. *N*-Acetylbenzotriazole was prepared by the method of Staab.⁷ The product had mp 49–50 °C (lit.⁷ 51 °C); IR 1735 cm^{-1} ($>\text{C}=\text{O}$, in CHCl_3 ; lit.⁸ 1735 cm^{-1}); UV (phosphate 0.1 M, pH 7.0) λ_{max} 219 nm (ϵ 14 400), 262.5 (7020), 297.5 (4620); ¹H NMR (CCl_4) 3.0 ppm (s, 3, CH_3), 7.5–8.4 ppm (m, 4, phenyl). Difluoroacetic acid, dichloroacetic acid, methoxyacetic acid, *n*-propylamine, and 2-methoxyethylamine were redistilled; disodium methylarsonate, methoxyamine hydrochloride, hydrazine dihydrochloride, glycine ethyl ester hydrochloride, 2,2,2-trifluoroethylamine hydrochloride, benzotriazole, and 3-quinuclidinol were recrystallized before use. Other reagents were commercial preparations. Acetonitrile was purified by the method of Coetzer.⁹ Buffers were prepared from reagent grade materials. The heavy water containing at least 99.95% D_2O was purchased from CEA France. Glass-distilled water was used throughout. The pK_a value of benzotriazole was determined by pH titration with standard sodium hydroxide.

Kinetic Measurements. Except for a few hydrolysis experiments carried out in a pH-stat Radiometer, Type TTT1c, reaction rates were

measured spectrophotometrically by following the disappearance of the absorption of *N*-acetylbenzotriazole at 300 nm on a Cary Model 15 spectrophotometer equipped with a thermostated cell holder. All runs were carried out at 25 °C, ionic strength maintained at 1.0 with potassium chloride. The solvent used for all the kinetic studies was 2.5% (v/v) acetonitrile–water. The pH was measured before and after each run using the pH-stat Radiometer equipped with a Type B glass electrode. A typical run using the concentration 2×10^{-4} M for *N*-acetylbenzotriazole and a given concentration of buffer and amine was performed as follows. Cells (1 cm) filled with 1 mL of a buffer or amine solution containing the appropriate potassium chloride concentration were equilibrated at 25.0 °C for 8–10 min. Dry acetonitrile (25 μL) was previously added to the reference cell. After temperature equilibrium, 25 μL of a *N*-acetylbenzotriazole stock solution in acetonitrile was introduced into the sample cell; the resulting solution was quickly mixed and the decreasing absorbance at 300 nm was followed. For experiments carried out in the presence of methoxyamine, a solution of methoxyamine was added to the buffer (final concentration 0.04 M) before the usual incubation, except for chloroacetate. In this case,³ to avoid the side reaction of methoxyamine with chloroacetate, no preincubation was performed. Faster reactions with hydrazine and 3-quinuclidinol were followed at 25.0 °C using a Durrum-Gibson Model 13001 stopped-flow spectrophotometer. The disappearance of *N*-acetylbenzotriazole was followed at 300 nm after mixing equal volumes of aqueous solutions of 2×10^{-4} M *N*-acetylbenzotriazole and 0.1–0.4 M hydrazine (or 0.1–0.4 M 3-quinuclidinol in the presence or absence of 0.08 M methoxyamine), both at ionic strength 1.0 M (KCl) and 2.5% (v/v) acetonitrile in order to minimize refractive index changes on mixing. Each rate measurement was repeated at least four times. Hydrolysis experiments carried out in the absence of external buffers were followed in a pH-stat assembly in the usual conditions using a 1×10^{-2} M *N*-acetylbenzotriazole aqueous solution. The pD values were taken as the pH meter readings plus the proper correction (0.41).¹⁰

All reactions were followed to completion under pseudo-first-order conditions. For spectrophotometric determinations, the corresponding rate constants (k_{obsd}) were obtained from least-squares analysis of plots of $\ln(\text{OD}_t - \text{OD}_\infty)/(\text{OD}_0 - \text{OD}_\infty)$ vs. time. Usually, the plots were linear to at least 4 half-lives; for stopped-flow experiments, deviations from linearity after 2–3 half-lives were observed. The reproducibility was within ± 2 –5%. All computations were carried out using a Diehl-Algotronic calculator.

Treatment of Kinetic Data. Above pH 2.5, the rate constants for the hydrolysis of *N*-acetylbenzotriazole in the absence of external

buffers are described by⁵

$$k_0 = k_w + k_{\text{OH}^-}[\text{OH}^-] \quad (1)$$

The rate constants for the base (k_{OH^-}) and the pH-independent (k_w) reactions were obtained from the slope and intercept of the plot of the pseudo-first-order rate constants (k_0) against hydroxide ion concentration, respectively. This concentration was calculated from the pH, $K_w = 10^{-14}$, and an activity coefficient for hydroxide ion¹¹ of 0.67.

For the disappearance of *N*-acetylbenzotriazole catalyzed by acetate, substituted acetate, phosphate, methylarsonate, carbonate, and 3-quinuclidinol buffers, linear plots of the pseudo-first-order rate constants, k_{obsd} , against total buffer concentration were found over the range 0.05–0.6 M buffer. Values of k_0 (s^{-1}) and k_{S}' ($\text{M}^{-1} \text{s}^{-1}$) were obtained from the intercepts and the slopes of these plots, respectively. Rate constants k_{B} for reaction with the basic species of the buffer and k_{BH^+} for reaction with the acid one (eq 10) were determined from the intercepts at 1.0 and 0.0, respectively, of plots of k_{S}' against the fraction free base of the buffer. When the same experiments were carried out in the presence of a constant concentration of added methoxyamine, the slopes of the linear plots of k_{obsd} against total buffer concentration were corrected by the corresponding value of k_{S}' . Plots of these corrected values divided by the concentration of free methoxyamine, (k_{cat}), against the fraction free base of the buffer led to the determination of the rate constants k_3 ($\text{M}^{-2} \text{s}^{-1}$) for catalysis of methoxyaminolysis by the basic component of the buffer and k_4 ($\text{M}^{-2} \text{s}^{-1}$) for catalysis by the acidic component³ (eq 10).

For reactions with primary amines, except *n*-propylamine, plots of $(k_{\text{obsd}} - k_0)/[\text{RNH}_2]_{\text{T}}$ against $[\text{RNH}_2]_{\text{T}}$ were found to be linear. The plots of the intercepts k_1 ($\text{M}^{-1} \text{s}^{-1}$) against the fraction of the amine in the basic form allow the determination of the k_1' and the k_2' terms ($\text{M}^{-1} \text{s}^{-1}$) of eq 11.^{12,13} By plotting the slopes k_{S} ($\text{M}^{-2} \text{s}^{-1}$) divided by the fraction free base of the amine against this fraction, the values of k_3 and k_4 ($\text{M}^{-2} \text{s}^{-1}$) were obtained from the intercepts at 1.0 and 0.0, respectively. For *n*-propylamine, the k_1' and k_2' terms were obtained from the intercepts at 1.0 and 0.0, respectively, of plots of the slopes k_{S}' (determined from the linear plots of k_{obsd} vs. $[\text{RNH}_2]_{\text{T}}$) against the fraction free base of the amine.

When the observed catalytic constant represented less than a 10% increase over the concentration range of buffer, it is reported as an upper limit corresponding to a 10% increase in rate at the largest buffer concentration. For catalysts in which the catalytic coefficient for one ionic species is much larger than that for the other, an upper limit was obtained by assuming a 10% error for the catalytic coefficient obtained at the highest or lowest fraction of free base.

Calculation of Theoretical Brønsted Plots. For the general base and the general acid catalysis of the methoxyaminolysis of *N*-acetylbenzotriazole, the Brønsted plots describing "Eigen curves" for simple proton transfer were calculated from the steady-state rate laws¹⁴

$$k_3 = \frac{K_{\text{add}}k_{\text{B}}k_{111}'k_{1\text{V}}'}{k_{111}'k_{1\text{V}}' + k_{-\text{B}}k_{1\text{V}}' + k_{-\text{B}}k_{-111}'} \quad (2)$$

$$k_4 = \frac{K_{\text{add}}k_{\text{HA}}k_{111}k_{1\text{V}}}{k_{111}k_{1\text{V}} + k_{-\text{HA}}k_{1\text{V}} + k_{-\text{HA}}k_{111}} \quad (3)$$

based on the elementary rate constants shown in Scheme III with $\text{R} = \text{CH}_3\text{O}$. $K_{\text{add}}k_{\text{B}}$ and $K_{\text{add}}k_{\text{HA}}$ are the limiting rate constants for diffusion-controlled encounter of T^\pm with the basic and the acid catalysts, respectively. The values of $k_{-\text{B}}$, $k_{-\text{HA}}$, $k_{1\text{V}}$, and $k_{1\text{V}}'$ for the separation of the encounter complexes between the catalysts and the tetrahedral intermediates were taken as 10^{11} s^{-1} .¹⁵ k_{111} , k_{-111} , k_{111}' , and k_{-111}' were calculated near the region of $\Delta\text{pK} = 0^{15}$ from $\log k_{111} (\text{s}^{-1}) = \log k_{111}' (\text{s}^{-1}) = 10 + 0.5\Delta\text{pK}$ and $\log k_{-111} (\text{s}^{-1}) = \log k_{-111}' (\text{s}^{-1}) = 10 - 0.5\Delta\text{pK}$ with $\Delta\text{pK} = \text{pK}_{\text{T}^\pm} - \text{pK}_{\text{HA}}$ for k_{111} and k_{-111} , and $\Delta\text{pK} = \text{pK}_{\text{BH}^+} - \text{pK}_{\text{T}^\pm}$ for k_{111}' and k_{-111}' .

The steady-state rate expressions for type II mechanism (see Discussion) are given by the equations

$$k_3 = \frac{K_{\text{add}}k_{\text{B}}k_{\text{c}}'}{k_{-\text{B}} + k_{\text{c}}'} \quad (4)$$

$$k_4 = \frac{K_{\text{add}}k_{\text{HA}}k_{\text{c}}}{k_{-\text{HA}} + k_{\text{c}}} \quad (5)$$

$$k_4 = \frac{K_{\text{add}}k_{\text{i}}k_{\text{j}}}{k_{-\text{i}} + k_{\text{j}}} \quad (6)$$

based on Scheme III.³ The calculation of the corresponding Brønsted plots was based on the Brønsted equations

$$\log k_{\text{c}}' = 0.59\text{pK}_{\text{a}} + 7.06 \quad (7)$$

$$\log k_{\text{c}} = -0.75\text{pK}_{\text{a}} + 14.8 \quad (8)$$

$$\log k_{\text{j}} = -0.75\text{pK}_{\text{a}} + 6.44 \quad (9)$$

for the concerted decomposition steps k_{c}' , k_{c} , and k_{j} , respectively. The value of $K_{\text{add}}k_{\text{i}}$ is the catalytic constant in the region of $\alpha = 0$. Based on the estimated values of pK_2 and pK_3 (next paragraph), the equilibrium constant $k_{\text{i}}/k_{-\text{i}}$ was calculated as $10^{6.4}$ and $k_{-\text{i}}$ was taken as $10^9/10^{6.4} \text{ M}^{-1} \text{ s}^{-1}$.

Estimation of pK Values. The pK_{a} of the tetrahedral addition intermediate T^\pm formed between *N*-acetylbenzotriazole and methoxyamine, and other equilibrium constants for protonic equilibria involving T^\pm (Scheme I with $\text{R} = \text{benzotriazole}$), may be derived from the estimated pK_{a} values given by Fox and Jencks³ for the corresponding tetrahedral intermediates involved in the 1-acetyl-1,2,4-triazole-methoxyamine reaction. Replacement of triazole ($\text{pK}_{\text{a}} = 10.1$) by benzotriazole ($\text{pK}_{\text{a}} = 8.32$) on the central carbon atom should give a $\Delta\text{pK}_{\text{a}}$ of ca. $-1.8/(2.5)^2 = 0.3$ for all the tetrahedral intermediates if the fall-off factor for transmission of substituent effects through carbon is taken as 2.5.¹⁶ Hence, the ionization constants for the tetrahedral intermediates involved in the *N*-acetylbenzotriazole-methoxyamine reaction are estimated to be $\text{pK}_1 = 1.4$, $\text{pK}_2 = 7.7$, $\text{pK}_3 = 12.6$, and $\text{pK}_4 = 6.2$. Log K_2 for the conversion of T^0 to T^\pm may be estimated from the relationship $\log K_2 = \text{pK}_1 - \text{pK}_2 = -6.3$.

Results

Uncatalyzed and Catalyzed Water Attack. In the present study, the rate constants for hydrolysis were obtained in three different ways (Table I¹⁷). In one set of experiments, the observed rate constants for hydrolysis were extrapolated to zero buffer concentration using acetate, substituted acetate, phosphate, methylarsonate, carbonate, and 3-quinuclidinol buffers. Alternatively, the rate constants were obtained directly in a pH-stat assembly or using 10^{-3} M HCl (DCl) solutions. Above pH 2.5, the pH-rate profile for hydrolysis of *N*-acetylbenzotriazole (Figure 1) in 1.0 M KCl at 25 °C was found to follow the rate law of eq 1 with $k_w = 8.00 \times 10^{-5} \text{ s}^{-1}$ and $k_{\text{OH}^-} = 2.9 \times 10^2 \text{ M}^{-1} \text{ s}^{-1}$ ($k_w = 1.23 \times 10^{-4} \text{ s}^{-1}$ and $k_{\text{OH}^-} = 5.6 \times 10^2 \text{ M}^{-1} \text{ s}^{-1}$ in 0.1 M KCl ⁵). Staab has previously reported a rate constant of $1 \times 10^{-4} \text{ s}^{-1}$ for the neutral hydrolysis of *N*-acetylbenzotriazole at 22 °C.⁷ The pH-independent reaction observed from pH 2.5 to 6 occurs with a large D_2O solvent isotope effect ($k_{\text{H}_2\text{O}}/k_{\text{D}_2\text{O}} = 3.0$, Table I¹⁷) and a large negative entropy of activation (ca. -43 eu , Table II¹⁷). The hydrolysis is also catalyzed by the acid and base species of buffers (Table III¹⁷). The catalytic rate constants k_{B} and k_{BH^+} (eq 10) are summarized in Table IV.

Buffer-Catalyzed Methoxyaminolysis. The methoxyaminolysis of *N*-acetylbenzotriazole is subject to both general acid and general base catalysis. The rate constants for these catalyzed reactions were obtained from the observed rate constants, k_{obsd} , for the disappearance of the reagent in the presence of methoxyamine and of a series of buffers. The experimental conditions and results are given in Table III.¹⁷ k_{obsd} was found to be related to the concentration of the basic and acidic species of the nucleophile (methoxyamine, methoxyammonium ion) and catalyst (B , BH^+) according to the equation

$$k_{\text{obsd}} = k_0 + k_{\text{B}}[\text{B}] + k_{\text{BH}^+}[\text{BH}^+] + k_1[\text{CH}_3\text{ONH}_2] + k_2[\text{CH}_3\text{ONH}_3^+] + k_3[\text{B}][\text{CH}_3\text{ONH}_2] + k_4[\text{BH}^+][\text{CH}_3\text{ONH}_2] \quad (10)$$

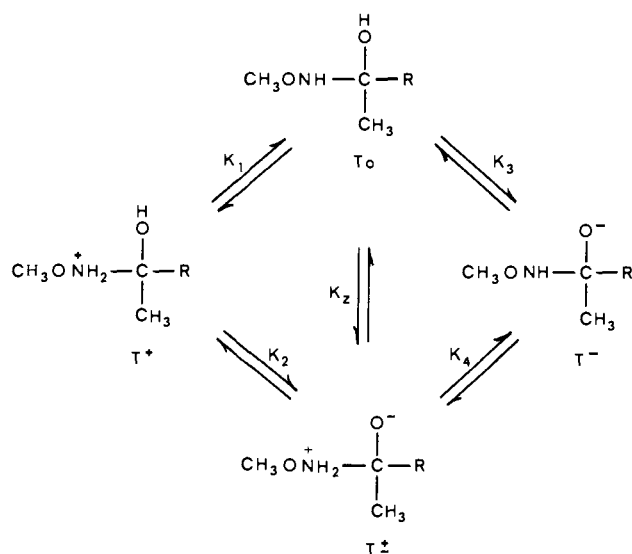
where k_0 is the hydrolysis rate in the absence of buffer. The derived rate constants are summarized in Table IV. By comparison with the rate constants k_3 and k_4 for catalysts of comparable pK , the catalytic rate constants for reactions with bicarbonate and methylarsonate monoanions may be attributed to an acid catalysis; phosphate monoanion may act as either a base or acid catalyst. Difluoroacetic and dichloroacetic acid show an extra term in the rate law given by $k_5[\text{BH}^+]$ -

Table IV. Summary of Derived Rate Constants for Reactions of *N*-Acetylbenzotriazole with Buffers in the Presence or Absence of Methoxyamine at 25 °C, Ionic Strength 1.0 M, 2.5% (v/v) Acetonitrile.

buffer	pK _a	k _B , M ⁻¹ s ⁻¹	k _{BH⁺} , ^a M ⁻¹ s ⁻¹	k ₃ , M ⁻² s ⁻¹	k ₄ , M ⁻² s ⁻¹
difluoroacetate (DFAA) ^b	1.05 ^c	1.6 × 10 ⁻⁵	1.0 × 10 ⁻⁴	1.0 × 10 ⁻³ ^d	3.7
dichloroacetate (DCAA) ^b	1.12 ^c	1.92 × 10 ⁻⁵	1.02 × 10 ⁻⁴	1.0 × 10 ⁻³ ^d	4.2
chloroacetate (CAA)	2.65 ^c	8.70 × 10 ⁻⁵	2.20 × 10 ⁻⁵	1.0 × 10 ⁻²	1.8
methoxyacetate (MAA)	3.33 ^c	1.52 × 10 ⁻⁴	1.50 × 10 ⁻⁵	3.7 × 10 ⁻²	2.75
acetate (AA)	4.60 ^c	3.44 × 10 ⁻⁴	0.44 × 10 ⁻⁵	2.8 × 10 ⁻¹	1.54
phosphate (P)	6.49 (1.72) ^c	3.7 × 10 ⁻³		3.2	0.34
methylarsonate (M)	8.50 (3.98) ^c	3.17 × 10 ⁻¹		3.25	3.0 × 10 ⁻² ^d
carbonate (C)	9.78 ^c	1.96 × 10 ⁻¹		7.75	2.0 × 10 ⁻³ ^d
3-quinuclidinol (QDL)	10.20 ^e	1.67		8.4	1.0 × 10 ⁻³ ^d

^a k_{BH⁺} was not detected for acids weaker than acetic acid. ^b These species showed an extra term in the rate law given by k₅[BH⁺][CH₃ONH₂][H⁺]; see text. ^c Fox, J. P.; Jencks, W. P. *J. Am. Chem. Soc.* **1974**, *96*, 1436–1449. ^d Upper limit only; see Experimental Section. ^e Page, M. I.; Jencks, W. P. *J. Am. Chem. Soc.* **1972**, *94*, 8828–8838.

Scheme I



[CH₃ONH₂][H⁺] with k₅ equal to 200 and 197 M⁻¹ s⁻¹, respectively.

Variation of Attacking Amine. The reactions of *N*-acetylbenzotriazole with amines follow the rate law^{3,12,13}

$$k_{\text{obsd}} = k_0 + k_1'[\text{RN}<] + k_2'[\text{RNH}^+<] + k_3'[\text{RN}<]^2 + k_4'[\text{RN}<][\text{RNH}^+<] \quad (11)$$

In contrast with the aminolyses of acetylimidazole¹³ and 1-acetyl-1,2,4-triazole,³ no catalysis by hydroxide ion was detected. The experimental conditions for the rate measurements and the derived rate constants are given in Table V.¹⁷ Second-order (k₁, k₂) and third-order (k₃, k₄) rate constants of eq 11 are summarized in Table VI. The nucleophilic reactions of amines with *N*-acetylbenzotriazole are moderately sensitive to intermolecular general base catalysis (k₃); this reaction path is nonexistent for *n*-propylamine and 3-quinuclidinol. Specific and general acid catalysis (k₂ and k₄, respectively) are rare and detectable only for hydrazine and weakly basic amines.

Discussion

Hydrolysis. As for 1-acetyl-1,2,4-triazole³ and esters of 1-hydroxybenzotriazole,¹⁸ the pH-rate profile for the hydrolysis of *N*-acetylbenzotriazole exhibits a substantial region where water is the dominant catalyst (Figure 1) with rate constants, k_w and k_{OH⁻}, which are slower than that obtained for 1-acetyl-1,2,4-triazole reactions. The observed isotope effect of ca. 3.0 for the pH-independent hydrolysis of *N*-acetylbenzotriazole suggests that at least two water molecules

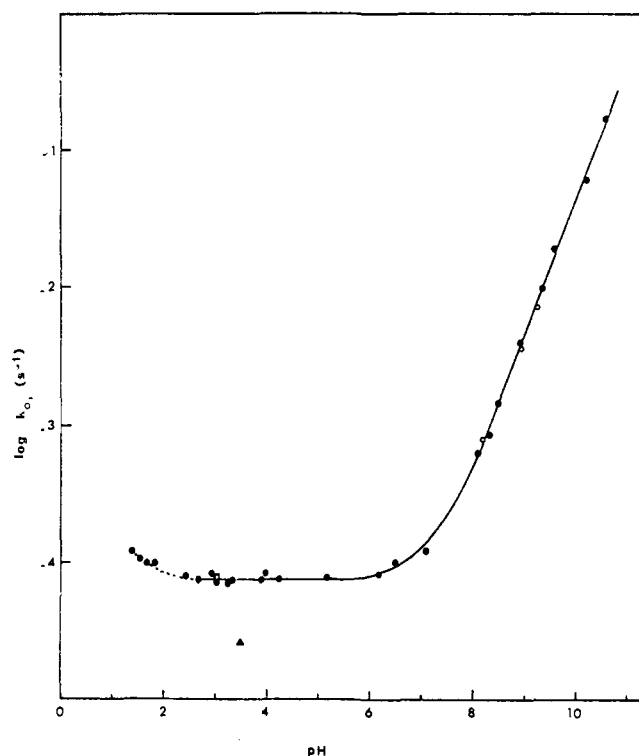


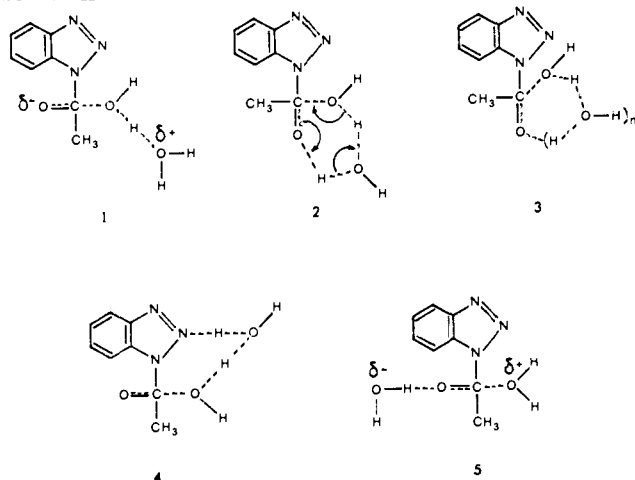
Figure 1. pH-rate profile for the hydrolysis of *N*-acetylbenzotriazole at 25 °C in 2.5% (v/v) acetonitrile, ionic strength 1.0 M (KCl). Rate measurements were extrapolated to zero buffer concentration (●); other measurements were made in 10⁻³ M HCl (□) and DCl (▲) solutions or using a pH-stat equipment (○). Above pH 2.5, the solid line was generated from eq 1 with k_w = 8.00 × 10⁻⁵ s⁻¹ and k_{OH⁻} = 2.9 × 10² M⁻¹ s⁻¹. The dashed line follows experimental points.

are bound in the transition state.¹⁹ This hypothesis is also supported by the large negative entropy of activation (ca. -43 eu). Furthermore, since water falls on the Brønsted line for general base catalysis (see below, Figure 2), it must act as a general base toward water, thus requiring a minimum of two water molecules in the activated complex. Likely depictions of the transition state, **1–5**, illustrating only the principal reactant water molecules are shown in Scheme 11. Noncyclic mechanism **1** is supported by the fact that water falls on the Brønsted line of Figure 2 (and not above that line as expected for cyclic mechanisms **2**, **3**, and **4**). Recent studies based essentially on Brønsted plots and proton inventories provide evidence for the involvement of transition-state structures similar to **1** (Scheme 11) in the water-catalyzed hydrolysis of esters, amides, and carbonates.²⁰ Structures similar to **5** can be ruled out by noting that the value for water is well removed from the

Table VI. Summary of Rate Constants for Reactions of Amines with *N*-Acetylbenzotriazole at 25 °C, Ionic Strength 1.0 M (KCl), 2.5% (v/v) Acetonitrile

amine	p <i>K</i> _a	<i>k</i> ₁ ' M ⁻¹ s ⁻¹	<i>k</i> ₂ ' M ⁻¹ s ⁻¹	<i>k</i> ₃ ' M ⁻² s ⁻¹	<i>k</i> ₄ ' M ⁻² s ⁻¹
methoxyamine (MA)	4.72 ^a	1.48 × 10 ⁻²	1 × 10 ⁻⁴	2.90 × 10 ⁻¹	1.275
2,2,2-trifluoroethylamine (TFE)	5.81 ^a	4.22 × 10 ⁻⁴		2.62 × 10 ⁻²	7.10 × 10 ⁻³
ethyl glycinate (EG)	7.90 ^b	3.68 × 10 ⁻²		1.38	
hydrazine (H)	8.20 ^c	3.17	1.2 × 10 ⁻¹	900	45
glycylglycine (GG)	8.25 ^b	1.36 × 10 ⁻¹		2.82	
2-methoxyethylamine (MEA)	9.72 ^b	3.02		66	
glycine (G)	9.76 ^b	3.33		62.6	
allylamine (A)	10.02 ^d	5.24		155	
3-quinuclidinol (QDL)	10.20 ^e	1.67			
<i>n</i> -propylamine (PA)	10.89 ^b	8.5			

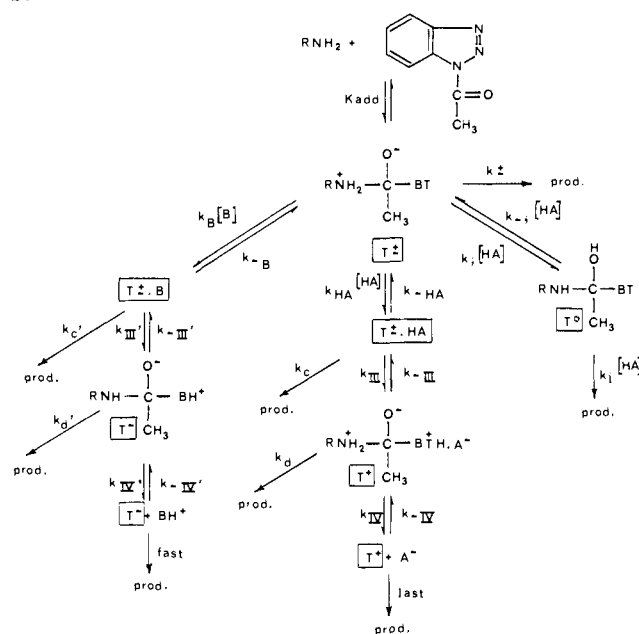
^a St Pierre, T.; Jencks, W. P. *J. Am. Chem. Soc.* **1968**, *90*, 3817–3827. ^b Jencks, W. P.; Gilchrist, M. *Ibid.* **1968**, *90*, 2622–2637. ^c Bruice, T. C.; Donzel, A.; Huffman, R. W.; Butler, A. R. *Ibid.* **1967**, *89*, 2106–2121. ^d Page, M. I.; Jencks, W. P. *Ibid.* **1972**, *94*, 3263–3264. ^e *Ibid.* **1972**, *94*, 8828–8838.

Scheme II

Brønsted line (slope = -0.4) for catalysis of hydrolysis by acids (see below).

The statistically corrected rate constants for the reactions of the basic component of the buffers with *N*-acetylbenzotriazole are displayed in Figure 2 on a Brønsted plot ($\beta = 0.38$) which intercepts the steeper line obtained for the uncatalyzed aminolysis near the phosphate point. The reactions of weak bases with the reagent may be attributed to general base catalysis of hydrolysis rather than to nucleophilic catalysis, based on the following observations: (1) the reactions of acetate and water exhibit solvent deuterium isotope effects equal to 2.2 (Table III¹⁷) and 3.0 (Table I¹⁷), respectively, as expected for general base catalysis;¹⁹ (2) the Brønsted value of 0.38 can be related to the β values of 0.34, 0.36, and 0.55 for the general-base-catalyzed hydrolysis of acetylimidazolium ion,¹³ 1-acetyl-1,2,4-triazole,³ and acetylimidazole,¹³ respectively. The positive deviations of the points for methylarsonate, carbonate, and hydroxide anions may represent nucleophilic reactions.

The rate constants corresponding to the rate accelerations of the disappearance of *N*-acetylbenzotriazole due to acetic acid and stronger carboxylic acids fall on a Brønsted plot of slope -0.4 (not shown). These reactions with acids may be accounted for¹³ by general acid catalysis of hydrolysis or by the kinetically equivalent reaction of *N*-acetylbenzotriazolium ion with the conjugate base of the acid, acting either as a nucleophilic reagent or a general base. The former pathway may be favored because *N*-acetylbenzotriazole exhibits little susceptibility to specific acid catalysis (pH-independent region extending down to pH 2.5, Figure 1). This can be related to the low p*K*_a (0.4²²) of benzotriazolium ion.

Scheme III

Catalyzed Methoxyaminolysis. The Brønsted plots for general acid and general base catalysis of the methoxyaminolysis of *N*-acetylbenzotriazole are shown in Figures 3 and 4, respectively. The rate constants in these figures are not statistically corrected in order to allow comparison with the Brønsted curves obtained in the 1-acetyl-1,2,4-triazole-methoxyamine reaction. The claim for nonlinearity of the Brønsted plot for base catalysis (Figure 4) is based on the small slope ($\beta \leq 0.1$) for catalysis by oxygen dianions and 3-quinuclidinol compared to the steeper slope ($\beta \geq 0.65$) for catalysis by weaker bases, carboxylate monoanions in particular. The catalytic constants for methoxyamine and 3-quinuclidinol are similar to those for oxygen anions of comparable basicity. Methylarsonate and carbonate monoanions show negative deviations from the line defined by carboxylate anions. A positive deviation is observed for phosphate monoanion. For general acid catalysis (Figure 3), the Brønsted plot undergoes a transition from a slope ≤ 0.1 for carboxylic acids to a slope ≥ 0.7 for weaker acids. The catalytic constants for methoxyammonium ion is similar to that observed for carboxylic acids. The limiting rate constants for catalysis by strong acids ($3.55 \text{ M}^{-2} \text{ s}^{-1}$) and strong bases ($6.3 \text{ M}^{-2} \text{ s}^{-1}$) are of the same order of magnitude. In both pathways, it is noteworthy (Figures 3 and 4) that the Brønsted plots are situated below the curved plots reported by Fox and Jencks³ for the general acid and the

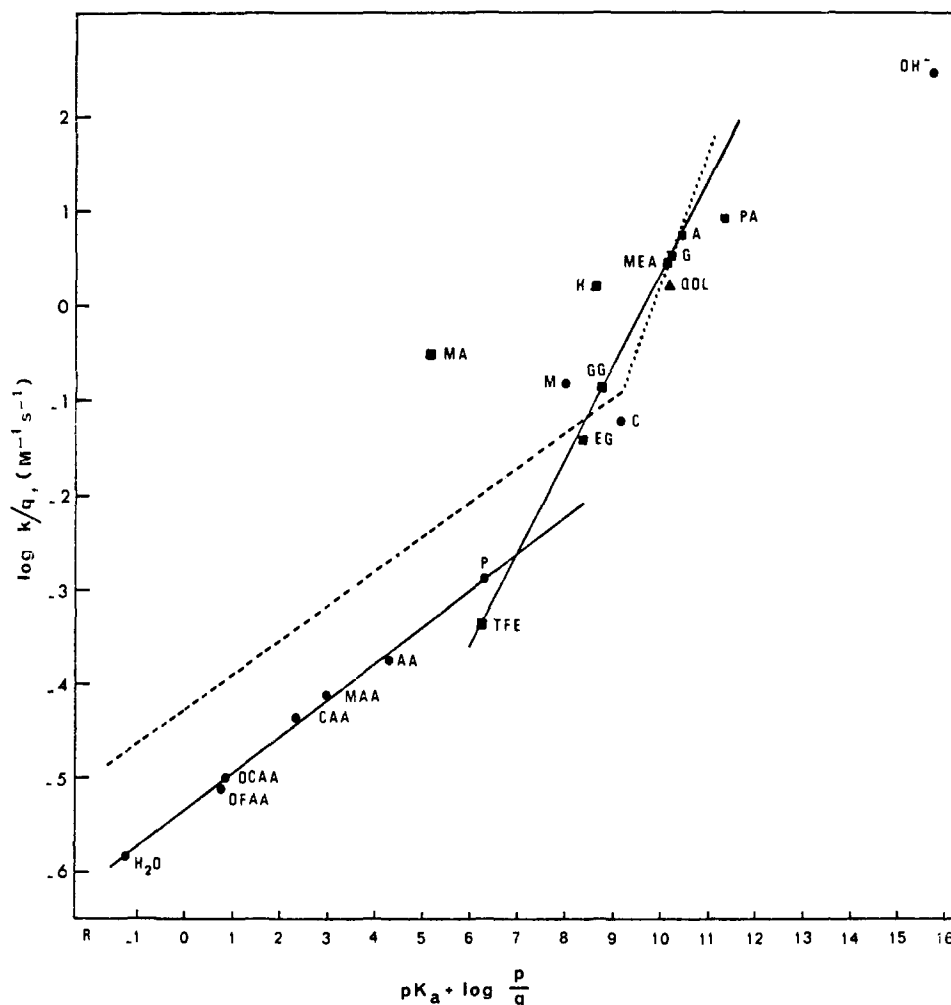


Figure 2. Rate constants for the reactions of buffer bases and nucleophiles with *N*-acetylbenzotriazole as a function of basicity at 25 °C, ionic strength 1.0 M (KCl), 2.5% (v/v) acetonitrile: (●) oxy anions, (■) primary amines, and (▲) 3-quinuclidinol. Statistical corrections have been made according to Bell and Evans.²¹ The abbreviations are identified in Tables IV and VI. The dashed line and the dotted line correspond to the Brønsted plots reported by Fox and Jencks³ for the general base catalysis of hydrolysis of 1-acetyl-1,2,4-triazole and for its uncatalyzed aminolysis, respectively (25 °C, ionic strength 1.0 M).

general base catalysis of the methoxyamine-acetyltriazole reaction (with negative deviations ~20- and 100-fold for strong and weak bases, respectively, and ~35- and 5-fold for strong and weak acids, respectively).

Once again, the nonlinear Brønsted plots support the occurrence of stepwise reaction mechanisms in both studied catalyzed pathways. They offer convincing evidence for the conclusion that an intermediate is not at equilibrium with respect to proton transfer.^{2a,23} Such nonlinear plots may be characteristic of proton-transfer reactions, the rate of which approach the diffusion-controlled limit (k_B or k_{HA} for base or acid catalysis, Scheme III) when the proton donor is a stronger acid than the conjugate acid of the proton acceptor and reach a limiting slope of 1 in the thermodynamically unfavorable direction (k_{-IV}' or k_{-IV} , Scheme III). For catalysts of intermediate strength, the rate-determining step is k_{III}' or k_{III} . For this mechanism, noted mechanism I, the break in the curve is expected to occur near the point at which the pK_a values of the proton donor and acceptor are equal.²⁴ The estimated pK_a value of $T^\pm = 6.2$ (see Experimental Section) is 1.3 unit above the break point at 4.9 for general base catalysis. For acid catalysis, protonation may occur either on the benzotriazole moiety or on the oxygen; the break point in the Brønsted plot at $pK = 6.5$ occurs at least 5 units above the expected pK_a of protonated benzotriazolium²² and 1.2 unit below the estimated pK_a of the hydroxyl group ($pK_2 = 7.7$). Mechanism I may

account for general acid and general base catalysis of the studied reactions considering the following features: (a) the experimental points fit the curvature actually observed for simple proton transfer with limiting slopes approaching 0 and 1;²⁴ (b) the proton shows a positive deviation of 54-fold from the Brønsted plot of Figure 3 which is of the order of magnitude (10–50-fold) that is required for diffusion-controlled proton transfer²⁴ (on the contrary, the third-order rate constant for the “water” reaction of methoxyamine with *N*-acetylbenzotriazole shows a positive deviation of 160-fold from the Brønsted plot of Figure 4 as would be expected if it occurred through a different mechanism); (c) with respect to the charges of the reacting species involved in the encounter processes (symmetrical or unsymmetrical nature) the position of the break may differ from $\Delta pK = 0$ by over 1 pK unit in the unsymmetrical cases,²⁴ and the pK_a values for T^\pm and T^+ are estimated with uncertainty (see Experimental Section). Nevertheless, general acid catalysis proceeding through mechanism I with protonation of the benzotriazole moiety is excluded by the large discrepancy (about 5 pK_a units) observed between the pK_a of the break point and that expected for protonated benzotriazole.

If the difference of 1.2 unit between the break point and the pK_a of the concerned tetrahedral intermediate is considered significant, more complex proton-transfer mechanisms may be envisaged.³ According to type II mechanisms (Scheme III),

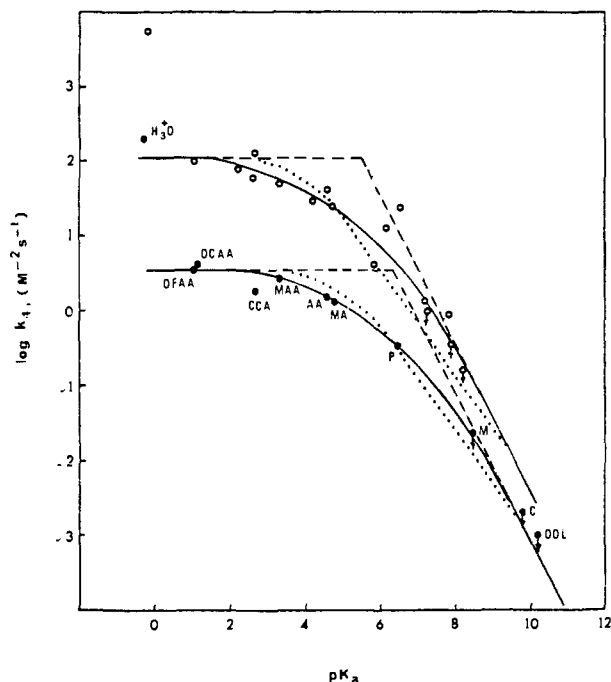


Figure 3. Brønsted plot for the general acid catalysis of the methoxyaminolysis of *N*-acetylbenzotriazole at 25 °C, ionic strength 1.0 M (KCl), 2.5% (v/v) acetonitrile (●). Upper limits for the rate constants are indicated by arrows. The broken line shows the limiting slopes of 1.0 and 0 obtained from the fit of the data to the Brønsted curve for a simple diffusion-controlled proton transfer (eq 3). The dotted line is the theoretical curve for the mechanism proceeding through k_c (Scheme III, eq 5). The Brønsted plot for general acid catalysis of the reaction of methoxyamine with 1-acetyl-1,2,4-triazole at 25 °C³ is shown (○).

the reaction occurs with strong catalysts at a diffusion-controlled rate but with weak catalysts at a slower rate assigned to a concerted general base (k_c' , mechanism II) or a concerted general acid (k_c , mechanism IIa) catalyzed decomposition of the addition tetrahedral intermediate T^\pm (if protonation by the acid occurs on the benzotriazole moiety). An alternative pathway for acid catalysis³ (mechanism IIb) corresponds to the general-acid-catalyzed breakdown of the uncharged tetrahedral intermediate T^0 rapidly formed from T^\pm which undergoes protonation on the oxygen and loss of a proton from the methoxyammonium group (Scheme III). The theoretical curves for general base catalysis (mechanism II) calculated from eq 4 and for general acid catalysis (mechanism IIa or IIb) calculated from eq 5 or 6, respectively, provide a satisfactory fit to the data (Figures 3 and 4). Type II mechanisms agree with the observed discrepancies between the position of the breaks in the Brønsted curves and the estimated pK_a of the intermediates since mechanisms II and IIb lower the pK_a at which the break occurs below that of T^\pm and of the hydroxyl group, respectively, while mechanism IIa raises the pK_a of the break above the pK_a of the protonated benzotriazole. A preassociation mechanism^{2b,25} can be ruled out by noting that it would lead to ΔpK_a discrepancies in the opposite direction. A preassociation mechanism has been described for the general acid catalysis of the methoxyaminolysis of phenyl acetate,²⁶ demonstrating a very short lifetime for the zwitterionic addition tetrahedral intermediate. The equilibrium constant K_{add} for the formation of T^\pm from methoxyamine and *N*-acetylbenzotriazole is approximately $3.5\text{--}6.3 \times 10^{-9} \text{ M}^{-1}$ if the limiting values k_{HA} or k_B are taken as $10^9 \text{ M}^{-1} \text{ s}^{-1}$.⁴ Hence the formation of T^\pm for this reaction is only slightly less favorable (~ 20 -fold) than that of the analogous intermediate involved in the methoxyamine-1-acetyl-1,2,4-triazole reaction ($K_{add} = 10^{-7} \text{ M}^{-1}$).³ For this latter reaction, it is suggested³ that T^\pm have a longer lifetime than T^- and T^+ since the results

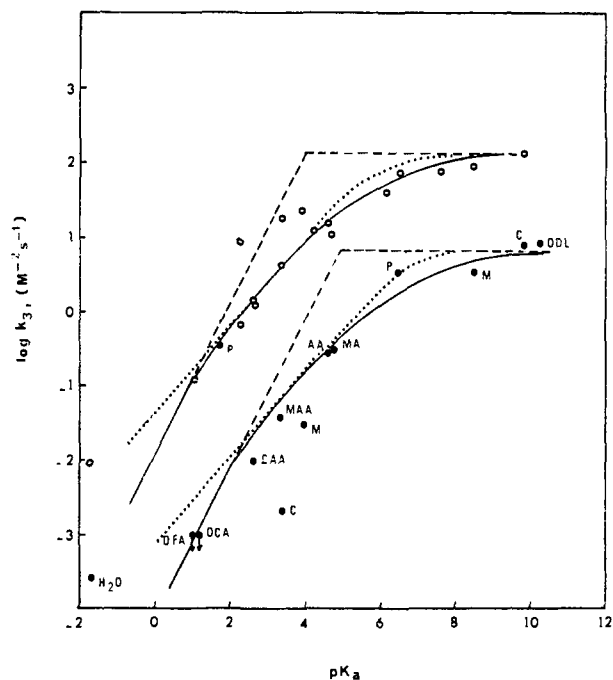


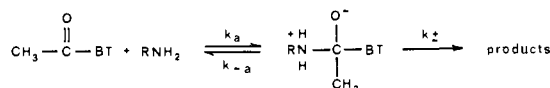
Figure 4. Brønsted plot for the general base catalysis of the methoxyaminolysis of *N*-acetylbenzotriazole at 25 °C, ionic strength 1.0 M (KCl), 2.5% (v/v) acetonitrile (●). Points for difluoroacetic (DFA) and chloroacetic (CA) acids are upper limits only. The broken line shows the limiting slopes of 1.0 and 0 obtained from the fit of the data to the Brønsted curve for a simple diffusion-controlled proton transfer (eq 2). The dotted line is the theoretical curve for the mechanism proceeding through k_c' (Scheme III, eq 4). The Brønsted plot for general base catalysis of the reaction of methoxyamine with 1-acetyl-1,2,4-triazole at 25 °C³ is shown (○).

obtained for the general acid and the general base catalyses are consistent with a type II mechanism. If T^- and T^+ have too short a lifetime to exist when they involve 1-acetyl-1,2,4-triazole, it appears reasonable that such "intermediates" T^- and T^+ do not exist in the methoxyamine-*N*-acetylbenzotriazole reaction since benzotriazole ($pK_a = 8.32$ at 25 °C, ionic strength 1.0 M KCl) and benzotriazolium ion ($pK_a = 0.422$) are better leaving groups than 1,2,4-triazole ($pK_a = 10.1$) and 1,2,4-triazolium ion ($pK_a = 2.6$). Finally, this last argument strongly supports type II mechanisms rather than type I mechanisms for reactions involving *N*-acetylbenzotriazole, if such concerted mechanisms are caused by the intermediates being too unstable to exist. Certainly in the *N*-acetylbenzotriazole case, the differences in the observed and calculated pK_a values are not large enough to prove type II mechanisms; nevertheless, the small discrepancies are in the right direction to make them more likely.

Uncatalyzed and Catalyzed Aminolysis. The Brønsted plot for the uncatalyzed aminolysis of *N*-acetylbenzotriazole (k_1' term, eq 11) is described by a slope ~ 1 (Figure 2). A small negative deviation from this line is observed for *n*-propylamine but it is less pronounced than that observed for the reactions of basic amines with esters and cationic amides.^{13,27,28} In these cases, the curvature of the Brønsted plot is interpreted in terms of a change in rate-determining step from rate-determining leaving group expulsion to rate-determining attack with most basic amines. The large positive deviations observed for methoxyamine and hydrazine can be attributed to an α -effect.

In most respects, the water-catalyzed aminolysis of *N*-acetylbenzotriazole conforms to the behavior of the previously studied reactions of amines and acyl compounds with good leaving groups: (a) the comparable reactivity of primary amines and 3-quinuclidinol means that no significant loss of a proton has occurred in the transition state;²⁷ (b) the observed

Scheme IV



β value is similar to that reported for class II reactions of most phenyl esters with amines ($\beta = 0.9 \pm 0.1$ ²⁹); (c) the point for *N*-acetylbenzotriazole falls close to the class II line in the sigmoid correlation of $\log k$ (uncatalyzed reaction) with the $\text{p}K_a$ of the leaving group obtained for the hydrazinolysis of alkyl and phenyl acetates²⁹ (not shown). Hence a similar mechanism (Scheme IV) is proposed to account for the uncatalyzed aminolysis of *N*-acetylbenzotriazole. The reaction pathway, involving a nonequilibrating zwitterionic tetrahedral intermediate whose breakdown through k^\ddagger is rate determining, is in agreement with the results obtained for the general base and the general acid catalysis of the methoxyaminolysis of the reagent since the catalyzed and the uncatalyzed reactions are observed simultaneously. A transition to rate-limiting attack of amine for the more basic *n*-propylamine may be envisaged by noting the absence of general base catalysis by a second molecule of amine for this reaction. The proposed mechanism of Scheme IV agrees with a transition state for the studied reactions at a similar or later point along the reaction coordinate than T^\ddagger .²⁹ On the contrary, product-like transition states have been suggested for acetylimidazole³⁰ and 1-acetyl-1,2,4-triazole³ reactions with amines based on the β values of 1.6 and 1.3, respectively. The present work establishes that a larger sensitivity to the basicity of the attacking amine is observed in the uncatalyzed aminolysis of *N*-acylazoles as the leaving group becomes poorer ($\text{p}K_{a, \text{L}} = 8.32, 10.1, \text{ and } 14.2$ for benzotriazole, 1,2,4-triazole, and imidazole, respectively).

The general base catalysis of aminolysis of *N*-acetylbenzotriazole is characterized by a linear Brønsted plot which gives a β value of 0.86 (Figure 5). This value, approaching the one (approximately 1.0) observed for the corresponding reactions with acetylimidazole,³¹ 1-acetyl-1,2,4-triazole,³ methyl formate,³² and phenyl acetate,³³ means that the sensitivity of these reactions to substituents on the amine is essentially the same as for protonation of the amine. This is in agreement with a rate-determining reaction of the intermediates T^\ddagger with the catalyzing amine in the transition state according to mechanism I (Scheme III, RNH_2 and RNH_3^+ instead of B and HA, respectively) or, if the tetrahedral intermediates T^- have a borderline existence, according to mechanism II (Scheme III).

Relative Leaving Group Abilities of Benzotriazole and Other Azoles. The results obtained in this work are of interest in relation to other studies involving *N*-acylazoles. Surprisingly, the absolute rate constants for all the studied reactions with *N*-acetylbenzotriazole are considerably slower than that expected from the $\text{p}K_a$ of benzotriazole. This phenomenon, previously noticed for 1-acetyl-1,2,4-triazole in comparison with acetylimidazole,³ is considerably emphasized by substituting the triazole moiety of 1-acetyl-1,2,4-triazole by benzotriazole. The Brønsted plots for the general base catalysis of the hydrolysis of *N*-acetylbenzotriazole (Figure 2), for its aminolysis catalyzed by a second molecule of amine (Figure 5), and for the general acid and the general base catalysis of its methoxyaminolysis (Figures 3 and 4) fall considerably below the Brønsted plots for the corresponding reactions with 1-acetyl-1,2,4-triazole. For the uncatalyzed aminolysis, the rate constants observed with *N*-acetylbenzotriazole are slightly faster (~ 1.7 -fold) for less basic amines and slightly slower (~ 2.5 -fold) for more basic ones than that obtained with 1-acetyl-1,2,4-triazole (Figure 2). This indicates that less pronounced discrepancies in the rates are observed for the uncatalyzed pathways than for the general-base- and -acid-cat-

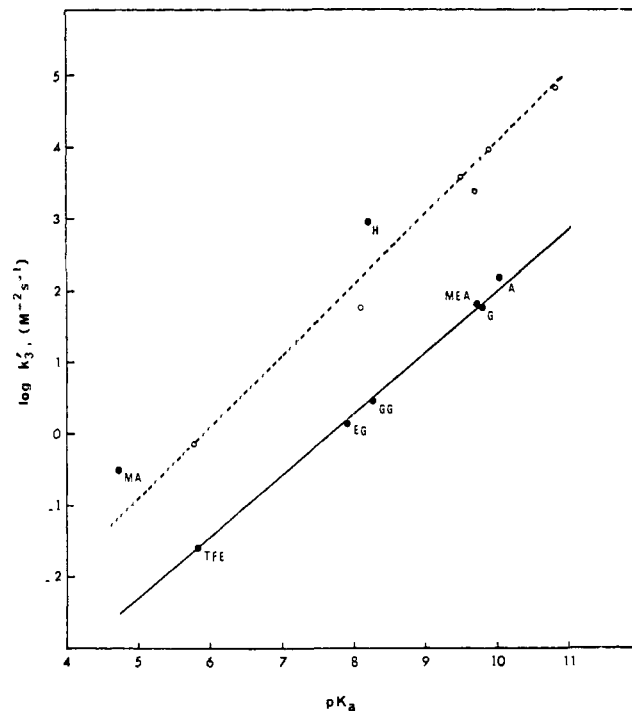


Figure 5. Dependence on amine $\text{p}K_a$ of the rate constants k_3' for the amine-catalyzed reactions of amines with *N*-acetylbenzotriazole at 25 °C, ionic strength 1.0 M (KCl), 2.5% (v/v) acetonitrile (—●—), and with 1-acetyl-1,2,4-triazole³ at 25 °C, ionic strength 1.0 M $(\text{CH}_3)_4\text{NCl}$ (---○---). The lines have a slope of 0.86 and 1.0, respectively.

alyzed ones. For example, the points for 2,2,2-trifluoroethylamine and allylamine show negative deviations of 50- and 320-fold, respectively, from the Brønsted lines of slope -0.5^3 describing $\log k_3'$ vs. $\text{p}K_a$ leaving group for the amine-catalyzed aminolysis of 1-acetyl-1,2,4-triazole and acetylimidazole.

Both mechanisms proposed to account for the results of the general acid and general base catalysis of the methoxyaminolysis of *N*-acetylbenzotriazole require that the rate-determining step is a diffusion-controlled encounter of strong acids and strong bases with T^\ddagger . The catalytic constants represent $K_{\text{add}}k_{\text{HA}}$ and $K_{\text{add}}k_{\text{B}}$, respectively (Scheme III), so that they are smaller than those obtained with 1-acetyl-1,2,4-triazole by the same factor as for the K_{add} values. If type II mechanisms are assumed for weak catalysts, the calculation of k_c' (eq 7) for a base catalyst of $\text{p}K_a = 6$, for example, leads to a value for this rate constant that is about three-fold smaller than for 1-acetyl-1,2,4-triazole reaction. Such a result is not consistent with the presumed better leaving ability of benzotriazole than of triazole anion. For an acid catalyst of $\text{p}K_a = 6$, the ratio obtained for the concerted breakdown of the tetrahedral addition intermediate (k_c , eq 8) is only about 3, favoring the reaction with *N*-acetylbenzotriazole. It appears that for weak catalysts the catalytic rate constants can be mostly determined by K_{add} (and K_{add} is less favorable for *N*-acetylbenzotriazole). This can hold also for mechanism I (eq 2 and 3) and for the aminolysis catalyzed by a second molecule of amine. On the contrary, the rates observed for the uncatalyzed aminolysis may be the result of an easier breakdown of T^\ddagger through k^\ddagger (Scheme IV) which can be helped by the lower $\text{p}K_a$ of benzotriazole. The general base catalysis of hydrolysis is characterized by an early transition state ($\beta = 0.38$) that must certainly involve no or little bond breaking of the leaving group. If a steric effect is involved, it would be small and the rate would not be decreased as observed in Figure 2. On the other hand, solvent effects are not sufficiently large to account for the values of the absolute rates obtained with *N*-acetylben-

zotriazole. Reactions were carried out in 0.03 and 2.5% acetonitrile for 1-acetyl-1,2,4-triazole and *N*-acetylbenzotriazole, respectively. A 5% decrease in rate constant k_w was observed upon the addition of 2.5% acetonitrile to the reaction with water in 10^{-3} M HCl at 25 °C. In fact, it can be simply suggested that the large differences in the behavior of *N*-acetylbenzotriazole and 1-acetyl-1,2,4-triazole may be accounted for by more stabilization of the ground state by resonance in the *N*-acetylbenzotriazole molecule than in the 1-acetyl-1,2,4-triazole one. It is well known that *N*-acylazoles are particularly reactive amides owing to the involvement of the electron pair of the amide nitrogen in the quasi-aromatic heterocyclic ring.⁸ However, *N*-acetylbenzimidazole, with a fused benzene ring, is notably less reactive than *N*-acetylimidazole.⁸ In spite of structures that are quite different for 1,2,3-triazole and 1,2,4-triazole, it is perhaps not unreasonable to underline the analogy of *N*-acetylbenzotriazole and 1-acetyl-1,2,4-triazole with these preceding compounds and to give a similar explanation for their relative reactivities. If there is less aromatic character or resonance in the heterocycle of the benzotriazole ring compared to 1,2,4-triazole (in particular, because it is conjugated with the fused benzene ring), this would free the lone pair electrons of the amide nitrogen for conjugation with the carbonyl group. There may also be effects due to variation in bond angles resulting from the fused rings.

Acknowledgment. We are greatly indebted to Professor M. Vilkas for his helpful advice and encouragement, and to Professor W. P. Jencks for his constructive comments and criticism of the manuscript. This work is a part of the thesis (CNRS A.O. 6151) submitted by M.R.R. in partial fulfillment of the requirements for Doctor of Science.

Supplementary Material Available: Experimental conditions and results of typical experiments (Tables I–III and V) (5 pages). Ordering information is given on any current masthead page.

References and Notes

(1) (a) Bruice, T. C.; Benkovic, S. J. "Bioorganic Mechanisms", Vol. I; W. A. Benjamin: New York, 1966. (b) Jencks, W. P. "Catalysis in Chemistry and

- Enzymology"; McGraw-Hill: New York, 1969. (c) Bender, M. L. "Mechanisms of Homogeneous Catalysis from Proton to Proteins"; Wiley-Interscience: New York, 1971.
- (2) (a) Jencks, W. P. *Chem. Rev.* **1972**, *72*, 705–718. (b) *Acc. Chem. Res.* **1976**, *9*, 425–432.
- (3) Fox, J. P.; Jencks, W. P. *J. Am. Chem. Soc.* **1974**, *96*, 1436–1449.
- (4) Page, M. I.; Jencks, W. P. *J. Am. Chem. Soc.* **1972**, *94*, 8828–8838.
- (5) Ravoux, M.; Laloi-Diard, M.; Vilkas, M. *Tetrahedron Lett.* **1971**, 4015–4018.
- (6) Reboud-Ravoux, M.; Ghelis, C. *Eur. J. Biochem.* **1976**, *65*, 25–33.
- (7) Staab, H. A. *Chem. Ber.* **1957**, *90*, 1320–1325.
- (8) Staab, H. A.; Rohr, W. In "Newer Methods of Preparative Organic Chemistry", Foerst, W., Ed.; Academic Press: New York, 1968; Vol. 5, pp 61–108.
- (9) Coetzee, J. F. *Prog. Phys. Org. Chem.* **1967**, *4*, 55–57.
- (10) Glasoe, P. K.; Long, F. A. *J. Phys. Chem.* **1960**, *64*, 188–190.
- (11) Kirsch, J. F.; Jencks, W. P. *J. Am. Chem. Soc.* **1964**, *86*, 833–837.
- (12) Jencks, W. P.; Carriuolo, J. *J. Biol. Chem.* **1959**, *234*, 1272–1279, 1280–1285.
- (13) Oakenfull, D. G.; Jencks, W. P. *J. Am. Chem. Soc.* **1971**, *93*, 178–188.
- (14) Gilbert, H. F. *J. Chem. Educ.* **1977**, *54*, 492–493.
- (15) Sayer, J. M.; Jencks, W. P. *J. Am. Chem. Soc.* **1973**, *95*, 5637–5649.
- (16) Wells, P. R. "Linear Free Energy Relationships"; Academic Press: New York, 1968; p 39.
- (17) See paragraph at end of paper regarding supplementary material.
- (18) McCarthy, D. G.; Hegarthy, A. F.; Hathaway, B. J. *J. Chem. Soc., Perkin Trans. 2*, **1977**, 224–231.
- (19) Anderson, B. M.; Cordes, E.; Jencks, W. P. *J. Biol. Chem.* **1961**, *236*, 455–463.
- (20) (a) Menger, F. M.; Venkatasubban, K. S. *J. Org. Chem.* **1976**, *41*, 1868–1870. (b) Hogg, J. L.; Phillips, M. K.; Jerkens, D. E. *Ibid.* **1977**, *42*, 2459–2461. (c) Hogg, J. L.; Phillips, M. K. *Tetrahedron Lett.* **1977**, 3011–3014. (d) Venkatasubban, K. S.; Davis, K. R.; Hogg, J. L. *J. Am. Chem. Soc.* **1978**, *100*, 6125–6128.
- (21) Bell, R. P.; Evans, P. G. *Proc. R. Soc. London, Ser. A* **1966**, *291*, 297–323.
- (22) Aten, W. C.; Büchel, K. H. *Z. Naturforsch. B* **1970**, *25*, 961–965.
- (23) Barnett, R. *Acc. Chem. Res.* **1973**, *6*, 41–46.
- (24) Eigen, M. *Angew. Chem., Int. Ed. Engl.* **1964**, *3*, 1–19.
- (25) Kerschner, L. D.; Schowen, R. L. *J. Am. Chem. Soc.* **1971**, *93*, 2014–2024.
- (26) Cox, M. M.; Jencks, W. P. *J. Am. Chem. Soc.* **1978**, *100*, 5956–5957.
- (27) Jencks, W. P.; Gilchrist, M. *J. Am. Chem. Soc.* **1968**, *90*, 2622–2637.
- (28) Fersht, A. R.; Jencks, W. P. *J. Am. Chem. Soc.* **1970**, *92*, 5442–5452.
- (29) Satterthwait, A. C.; Jencks, W. P. *J. Am. Chem. Soc.* **1974**, *96*, 7019–7031.
- (30) Page, M. I.; Jencks, W. P. *J. Am. Chem. Soc.* **1972**, *94*, 3263–3264.
- (31) Oakenfull, D. G.; Salvesen, K.; Jencks, W. P. *J. Am. Chem. Soc.* **1971**, *93*, 188–194.
- (32) Blackburn, G. M.; Jencks, W. P. *J. Am. Chem. Soc.* **1968**, *90*, 2638–2645.
- (33) Bruice, T. C.; Donzel, A.; Huffman, R. W.; Butler, A. R. *J. Am. Chem. Soc.* **1967**, *89*, 2106–2121.